

Ultimate strength of duplex stainless steel plates under uniaxial compression

This paper discusses the ultimate compressive strength of stainless steel plates made from JIS SUS329J3L duplex stainless steel (EN 1.4462). Firstly, based on coupon test results for SUS329J3L, the applicability of the existing constitutive equation for SUS329J3L is confirmed and the validity of a numerical analysis incorporating the equation shown in comparison with the results of compression testing for a stiffened stainless steel plate. Secondly, the ultimate compressive strength of simply supported plates and outstanding plates made from SUS329J3L is examined by way of a numerical analysis and compared with that of JIS SM570 structural carbon steel. Finally, the ultimate compressive strength of plates made from SUS329J3L is discussed in relation to existing ultimate strength curves.

1 Introduction

Many steel bridges in Japan were built in the 1960s and subsequent corrosion-related damage has made maintenance and repair work for existing structures an urgent issue. As stainless steel has a superior corrosion resistance and greater or equivalent tensile strength with respect to ordinary structural carbon steel, its use for bridge members is an attractive proposition. According to existing estimations [1], the total life cycle cost of a stainless steel footbridge on an oil platform is 0.55 times that of a carbon steel equivalent. Moreover, connection technologies for stainless steel members have also made progress in the construction of stainless steel road bridges [2].

Although many grades of stainless steel have been developed, the austenitic, ferritic and duplex types are the most suitable for everyday structural use. The austenitic grade has relatively favourable corrosion resistance, but the material costs involved are very high compared with those for structural carbon steel due to the high content of nickel – a rare element. Austenitic stainless steel has already been adopted as one type of architectural structural steel in Japan. The corrosion resistance of the ferritic grade is inferior to that of the austenitic type, but the associated material costs are lower because ferritic stainless steel contains chromium instead of nickel to improve cor-

rosion resistance. The duplex grade exhibits superior corrosion resistance and tensile strength to those of general stainless steel, but its material costs are extremely high when compared with other stainless steel types. In Japan JIS SUS329J3L stainless steel is developed as a duplex grade and – as shown in Table 1 – it has almost the same chemical composition as EN 1.4462.

In order to be able to use stainless steel for bridge members, design specifications are required; such specifications for the application of ordinary austenitic stainless steel in building structures have already been introduced in Japan [3]. However, Japan currently has no design specifications for the use of stainless steel for bridge members, although such specifications are in place in Europe and the USA. In Europe in particular, bridges with stainless steel main members have already been constructed [2]. Accordingly, in Japan a number of studies [4], [5], [6] dealing with the use of austenitic stainless steel for bridge members have recently been reported. In [4] a box-shaped hybrid girder consisting of a stainless steel flange plate and carbon steel ribs is proposed to reduce the initial costs of using stainless steel. In that study the weldability of the carbon steel ribs to the stainless steel flange panel and initial imperfections due to this welding were clarified by testing and numerical analyses. Refs. [5] and [6] report on the shear strength of stainless steel webs in I-shaped girders, and [7] clarifies the ductility and ultimate strength of ferritic stainless steel members with respect to reducing material costs through the use of ferritic stainless steel for structural members. However, under current conditions, the ductility and ultimate compressive strength of duplex stainless steel plates have not been sufficiently clarified to allow the use of duplex stainless steel for bridge members. Although this type of steel is given as an available grade in European design specifications [8], it has been pointed out that these provisions are not always effective for duplex stainless steel because they conform to the values of ordinary structural carbon steel or austenitic stainless steel [9].

In order to permit the use of JIS SUS329J3L duplex stainless steel for bridge members, this study aims to clarify the compressive behaviour and ultimate compressive strength of SUS329J3L plates. The authors propose a reliable constitutive equation for austenitic stainless steel [10] and its applicability to SUS329J3L [11] is confirmed. In this study a numerical analysis using a constitutive equa-

Received 4 September 2009, revised 10 February 2010,
accepted 15 February 2010

* Corresponding author: miyoshi@civil.eng.osaka-u.ac.jp

Table 1. Chemical composition

Steel	Element (%)								
	C	Si	Mn	P	S	Ni	Cr	Mo	N
JIS SUS329J3L	≤ 0.030	≤ 1.00	≤ 2.00	≤ 0.040	≤ 0.030	4.50–6.50	21.00–	2.50–3.50	0.08–0.20
EN 1.4462	≤ 0.030	≤ 0.030	≤ 2.00	≤ 0.035	≤ 0.015	4.50–6.50	21.00–	2.50–3.50	0.08–0.22

Table 2. Mechanical properties

Steel		Modulus of elasticity (N/mm ²)	Tensile strength (N/mm ²)	Elongation (%)	Poisson's ratio	0.2 % proof stress or yield stress (N/mm ²)	Yield ratio
JIS	EN						
SUS329J3L	1.4462	192000	746	48	0.22	528	0.71
SM570	–	205800	570	26	0.30	504	0.88
SUS304	1.4301	178000	697	71	0.30	259	0.37
SUS304N2	–	180000	716	67	0.30	396	0.55
SUS316	1.4401	179000	574	76	0.30	254	0.44
SUS410L	–	204000	487	39	0.30	361	0.74

tion was carried out to ascertain the ductility and ultimate compressive strength of simply supported and outstanding SUS329J3L plates. In the numerical analysis, the aspect ratios, slenderness parameters and magnitude of residual stress were set as analytical parameters, and the ductility and ultimate compressive strength of SUS329J3L plates were compared with those of structural carbon steel JIS SM570. Based on this comparison, the compressive behaviour and ultimate compressive strength of SUS329J3L plates could be clarified.

2 Mechanical properties of SUS329J3L

Table 2 shows the mechanical properties ascertained in previous coupon tests [10], [11], [12] involving SUS329J3L, SM570 and representative stainless steel types (JIS SUS304, SUS304N2, SUS316 and SUS410 L). The properties listed are the average values of test results in the rolling and transverse directions. The table shows that stainless steel exhibits a higher ductility than SM570. Moreover, the yield ratio of stainless steel is smaller than that of SM570, and the 0.2 % proof stress value of SUS329J3L almost corresponds to the yield stress of SM570.

3 Numerical analysis

The finite element method using an eight-node isoparametric shell element was employed in this study to ascertain the ultimate compressive strength of SUS329J3L and SM570 plates by numerical analysis. This method is based on updated Lagrangian formulation to allow consideration of geometric non-linearity. Moreover, an isotropic hardening rule, an associated flow rule and the *von Mises* yield function were assumed to deal with the elasto-plastic problem. In the numerical analysis, the compound *Ramberg-Osgood* curve (see section 3.1) was employed as a constitutive equation for SUS329J3L. The backward *Euler* scheme as the stress integration algorithm and a consistent tangent modular matrix [13] were employed to improve the convergence of the iterative calculation.

3.1 Constitutive equation

The authors have already proposed a reliable constitutive equation for austenitic stainless steel. This equation (Eq. (1)) is called the “compound *Ramberg-Osgood* curve” [10].

$$\varepsilon = \begin{cases} \frac{\sigma}{E} & (0 \leq \sigma < \sigma_p) \\ \frac{\sigma}{E} + 0.002 \frac{\sigma^n - \sigma_p^n}{\sigma_{0.2}^n - \sigma_p^n} & (\sigma_p \leq \sigma < \sigma_{0.2}) \\ \frac{\sigma}{E} + a\sigma + b + c \left(\frac{\sigma - \sigma_{0.2}}{\sigma_{10} - \sigma_{0.2}} \right)^m & (\sigma_{0.2} \leq \sigma) \end{cases} \quad (1)$$

Constants a, b and c in Eq. (1) are given in Eq. (2).

$$\begin{cases} a = \frac{0.002n\sigma_{0.2}^{n-1}}{\sigma_{0.2}^n - \sigma_p^n} \\ b = \varepsilon_{0.2} - \frac{\sigma_{0.2}}{E_{0.2}} \\ c = \varepsilon_{10} - \varepsilon_{0.2} - \frac{\sigma_{10} - \sigma_{0.2}}{E_{0.2}} \end{cases} \quad (2)$$

where

- σ stress
- ε strain
- E modulus of elasticity
- σ_p proportion limit (0.01 % proof stress in accordance with [8])
- n, m hardening parameters of the first and second curves respectively
- $\sigma_{0.2}$ 0.2 % proof stress
- $\varepsilon_{0.2}$ strain at 0.2 % proof stress
- ε_{10} 10 % strain (= 0.1)
- σ_{10} stress at 10 % strain
- $E_{0.2}$ tangent modulus at 0.2 % proof stress

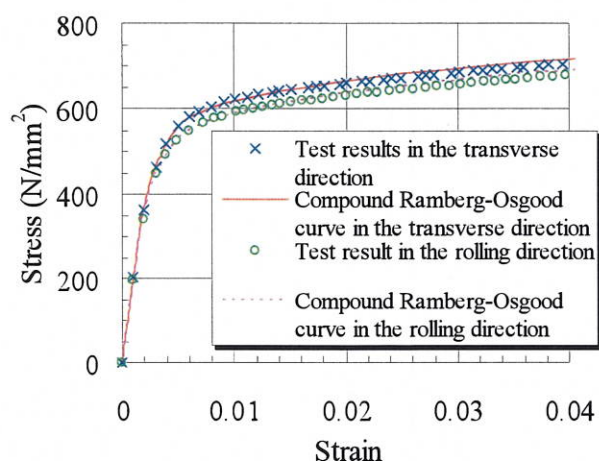


Fig. 1. Accuracy of the compound Ramberg-Osgood curve

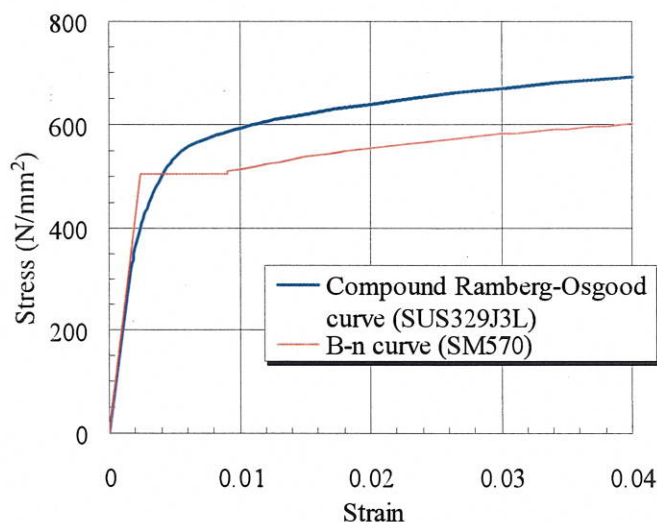


Fig. 2. Stress-strain curves in numerical analysis

Fig. 1 demonstrates the accuracy of the compound Ramberg-Osgood curve for the coupon test results [11] for SUS329J3L in the rolling and transverse directions respectively. It shows that the curve is applicable as a constitutive equation for SUS329J3L because the shapes are in good agreement with the test results. In the numerical analysis, the material constants of the curve were adopted with average values obtained from the coupon test results as shown in Table 3 (a). On the other hand, the B-n curve given by Eq. (3) [14] was employed as the constitutive equation for SM570.

$$\frac{\sigma}{\sigma_y} = \begin{cases} \varepsilon/\varepsilon_y & (0 \leq \varepsilon \leq \varepsilon_y) \\ 1.0 & (\varepsilon_y \leq \varepsilon \leq \varepsilon_H) \\ B(\varepsilon/\varepsilon_y)^n & (\varepsilon_H \leq \varepsilon) \end{cases} \quad (3)$$

where

σ_y yield stress

ε_y yield strain

ε_H strain at work-hardening initiation

B, n material constants representing the work-hardening area

Table 3. Material constants

(a) SUS329J3L

E (N/mm ²)	191,562
σ_p (N/mm ²)	316
$\sigma_{0.2}$ (N/mm ²)	528
$\varepsilon_{0.2}$	4.757×10^{-3}
σ_{10} (N/mm ²)	789
ε_{10}	9.991×10^{-2}
n	5.9
m	2.4
$E_{0.2}$ (N/mm ²)	34,817

(b) SM570

E (N/mm ²)	205,800
σ_y (N/mm ²)	504
ε_y	2.450×10^{-3}
ε_H	9.090×10^{-3}
B	0.8648
n	0.1152

The material constants of Eq. (3) are shown in Table 3 (b). Substituting these constants into Eqs. (1) and (3) produces the curves plotted in Fig. 2.

3.2 Validity of the numerical analysis

In order to verify the validity of the numerical analysis, an ultimate compressive strength analysis of a stiffened stainless steel plate was carried out, as shown in Fig. 3. The numerical results were compared with the test and FE analysis results of [4]. The compressive stiffened plate was made

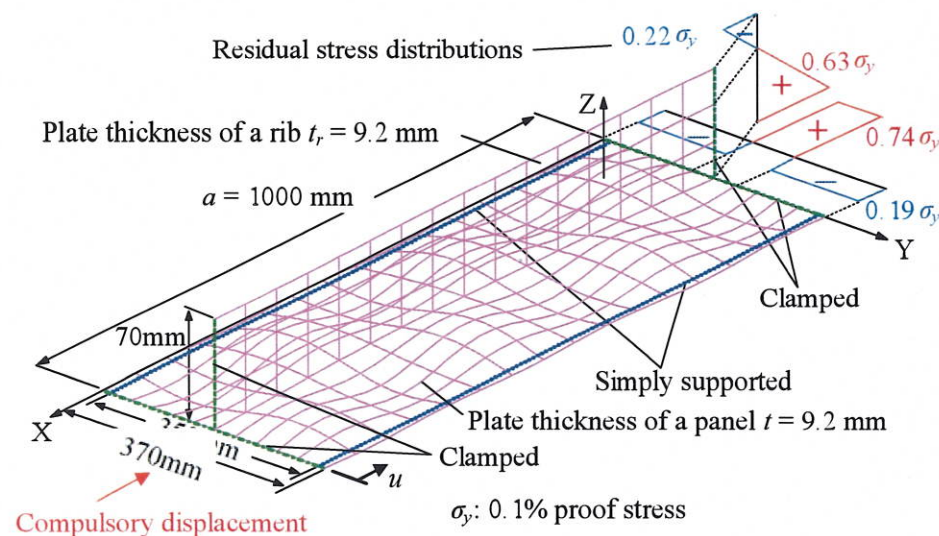


Fig. 3. Analytical model of a simply supported stiffened plate

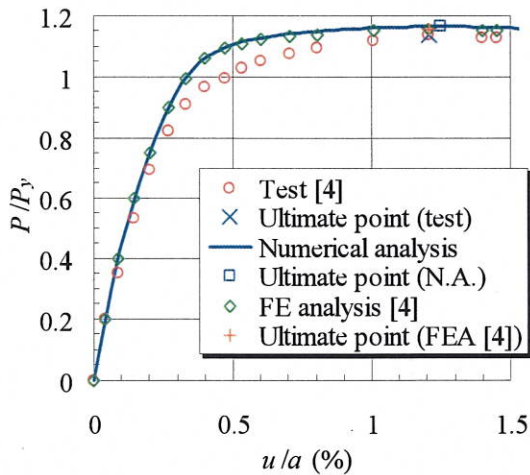


Fig. 4. Comparison between test and numerical analysis re-

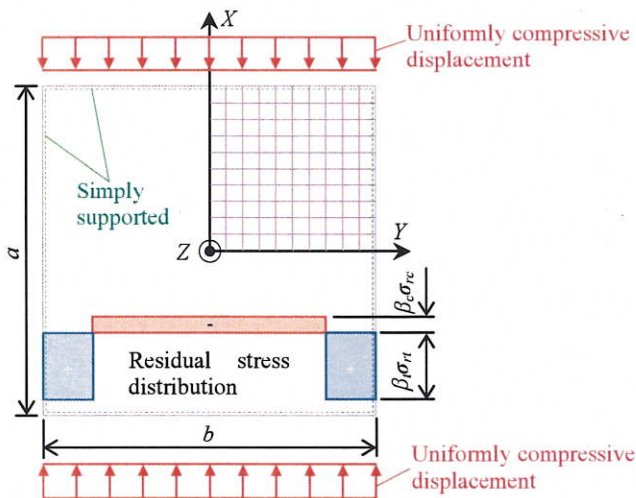


Fig. 5. Analytical model of simply supported plate

from JIS SUS304N2 A austenitic stainless steel, and the material constants of Eqs. (1) and (2) were determined from the coupon test results reported in [4].

Fig. 4 represents the relationships between the compression force and the average compressive strain of the stiffened plate. In Fig. 4, P is the compressive force and P_y is the yield axial force. From Fig. 4, since the curve and the ultimate point of the numerical analysis almost correspond to those of the test, and the numerical results are in good agreement with the FE analysis results of [4], it can be concluded that the numerical analysis method can be used for predicting the ultimate compressive behaviour of duplex stainless steel plates.

3.3 Analytical model of compressive plates

In this study, numerical analyses of simply supported and outstanding plates were conducted in order to ascertain the compressive behaviour and ultimate compressive strength of plates of SUS329J3L steel. The analytical models for these two types are outlined below.

3.3.1 Simply supported plates

A simply supported plate was adopted to represent plates in the cross-section of a compressive truss chord member, the

arch rib of an arch bridge, etc. [15]. In this study, the use of SUS329J3L for these elements was postulated, and focus directed on the basic compressive behaviour and ultimate compressive strength of simply supported SUS329J3L plates. In particular, the effects of aspect ratio and residual stress on the ultimate compressive strength of SUS329J3L plates are discussed here in comparison with those of SM570 plates because the 0.2 % proof stress of SUS329J3L almost corresponds to the yield stress of SM570.

As shown in Fig. 5, the analytical model for simply supported plates with width b and length a consisted of eight-node isoparametric finite elements and considered 1/4 symmetry.

The thickness of the simply supported plates was decided based on the slenderness parameter $\bar{\lambda}_p$ given in Eq. (4), assuming that the plate width b is constant.

$$\bar{\lambda}_p = \frac{b}{t} \sqrt{\frac{\sigma_F}{E} \frac{12(1-\nu^2)}{\pi^2 k}} \quad (4)$$

where

σ_F design strength ($\sigma_{0.2}$ for SUS329J3L and σ_y for SM570)

E modulus of elasticity

ν Poisson's ratio (0.3)

k buckling coefficient (4 is assumed as the constant value)

The shape of the initial deflection was conservatively assumed to be as shown in Eq. (5) because the lateral deflection of the integer number of the half-wave occurs in slender plates subjected to in-plane compression, and the number is close to the aspect ratio.

$$W_0 = W_{0\max} \cos\left(\frac{\pi}{a} X\right) \cos\left(\frac{\pi}{b} Y\right) \quad (5)$$

where $W_{0\max}$ is the maximum value of initial deflection at the centre of the plate, and the maximum permissible fabrication error $b/150$ specified in [16] is adopted.

3.3.2 Outstanding plates

The use of SUS329J3L for the flange plate of an I-shaped girder, the longitudinal rib of a stiffened plate subjected to compression, etc. [17] was assumed, and the basic compressive behaviour and ultimate compressive strength of outstanding SUS329J3L plates investigated. In particular, the effect of aspect ratio and residual stress on the ultimate compressive strength of SUS329J3L plates is discussed here in comparison with that of SM570 plates.

The analytical model for outstanding plates with length a and width b as shown in Fig. 6 consisted of eight-node isoparametric finite elements with half symmetry as shown in Fig. 7. The plate thickness t of the outstanding plates was obtained from Eq. (4), substituting 0.425 for the buckling parameter k .

The initial deflected shape of the outstanding plates was assumed as per Eq. (6), and the maximum value $W_{0\max}$ in Fig. 6 was adopted for the maximum permissible fabrication error $b/100$ specified in [16].

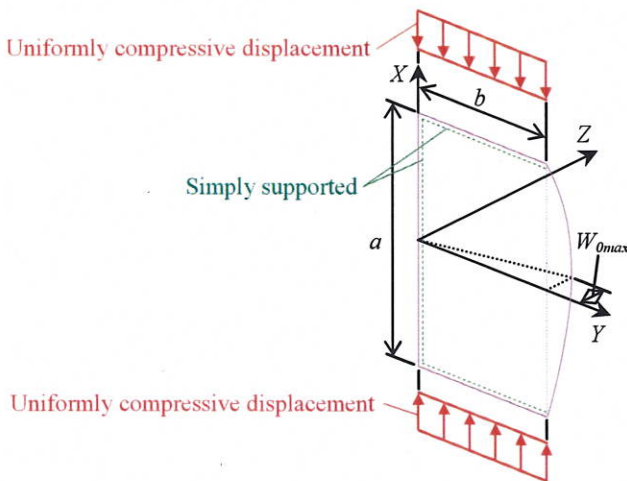


Fig. 6. Initial deflected shape of outstanding plate

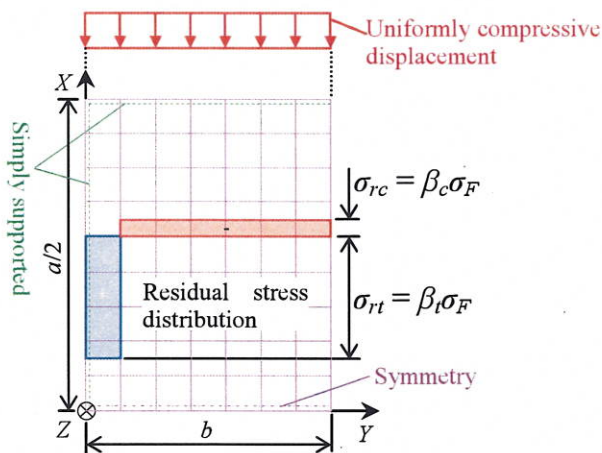


Fig. 7. Analytical model of outstanding plate

$$W_0 = W_{0max} \frac{Y}{b} \cos\left(\frac{\pi X}{a}\right) \quad (6)$$

3.4 Analytical parameters

The analytical parameters were decided based on existing studies [15] and [17] with regard to the ultimate compressive strength of structural carbon steel plates. In this study the aspect ratio α ($=a/b$), the slenderness parameter $\bar{\lambda}_p$ and the magnitude of the tensile residual stress of SUS329J3L plates were set as parameters.

3.4.1 Simply supported plates

In order to ascertain the minimum ultimate compressive strength of simply supported plates, $\alpha = 0.25, 0.50, 0.75$ and 1.00 , and $\bar{\lambda}_p = 0.5, 0.7, 0.9$ and 1.1 were set as analytical parameters. The shape of the residual stress distribution was rectangular (as shown in Fig. 5) in order to satisfy the self-equilibrium condition, and the magnitude of the compressive residual stress σ_{rc} was 0.2 times the value of $\sigma_{0.2}$ or σ_y . The tensile residual stress σ_{rt} of SUS329J3L plates was assumed to be 0.9 or 1.0 times the value of $\sigma_{0.2}$,

and that of SM570 plates 0.9 times the value of σ_y . Although the residual stress of SUS329J3L welded plates has not yet been clarified, the aforementioned shape and magnitude of residual stress for such plates were decided based on residual stress distribution models of plate-welded structures consisting of JIS SUS304N2 A austenitic stainless steel [18] and SM570 [19] because the metallographic structure and thermo-mechanical characteristics of SUS329J3L are considered to exhibit intermediate values between those of SM570 and those of austenitic stainless steel.

3.4.2 Outstanding plates

In order to ascertain the minimum ultimate compressive strength of outstanding plates, $\alpha = 1.0, 2.0, 3.0, 4.0, 5.0$ and 6.0 , and $\bar{\lambda}_p = 0.5, 0.7, 0.9, 1.1$ and 1.3 were set as analytical parameters. The shape of the residual stress distribution was rectangular (as shown in Fig. 7), as was the case with simply supported plates. In Fig. 7 compressive residual stress along the unsupported edge of the plate was assumed because gas cutting cannot be used for stainless steel containing $\geq 10\%$ chromium; ordinary shear cutting is therefore required. On the other hand, although gas cutting is generally available for SM570, in this study it was assumed that the unsupported edge of outstanding SM570 plates was shear-cut in order to clarify the ultimate compressive strength under the same conditions of residual stress as SUS329J3L and SM570.

4 Analytical results and discussion

The effects of residual stress, aspect ratio α and slenderness $\bar{\lambda}_p$ parameter on the compressive behaviour and ultimate compressive strength of simply supported and outstanding plates made from SUS329J3L are considered in comparison with those of SM570.

4.1 Effect of residual stress

The effect of the difference in residual stress distribution on the compressive behaviour of simply supported and outstanding plates made from SUS329J3L is discussed below.

4.1.1 Simply supported plates

The relationships between the non-dimensional average stress σ/σ_F and the non-dimensional average strain ϵ/ϵ_F of simply supported SUS329J3L plates with values of $\bar{\lambda}_p = 0.7$ and 0.9 , $\alpha = 1.0$, and $\sigma_{rt} = 0.9\sigma_{0.2}$ and $1.0\sigma_{0.2}$ are shown in Fig. 8 (a), where σ is the average compressive stress, ϵ is the average strain and ϵ_F is the strain at the design strength.

This figure indicates that the non-dimensional average stress-strain curves of plates with $\sigma_{rt} = 0.9\sigma_{0.2}$ correspond to those with $\sigma_{rt} = 1.0\sigma_{0.2}$. Moreover, it is confirmed that the difference in residual stress scarcely affects the compressive behaviour of all plates except those that also have values of $\bar{\lambda}_p = 0.7$ and 0.9 and $\alpha = 1.0$. Thus, the value of $\sigma_{rt} = 0.9\sigma_{0.2}$ has been adopted for simply supported SUS329J3L plates in the discussion.

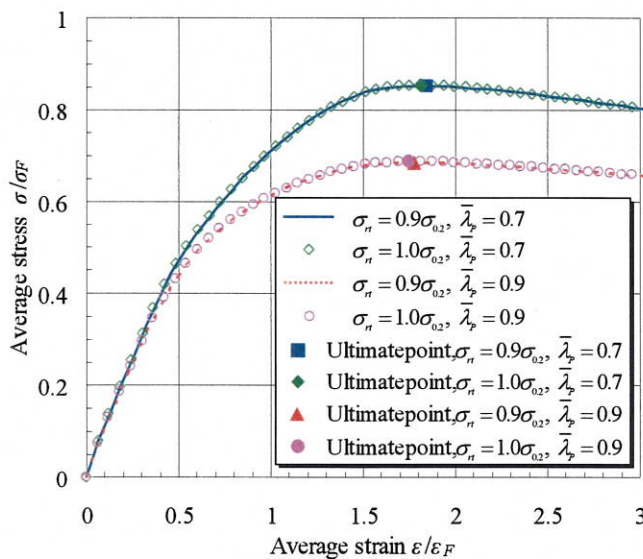
4.1.2 Outstanding plates

The relationships between the non-dimensional average stress σ/σ_F and the non-dimensional average strain $\varepsilon/\varepsilon_F$ for outstanding SUS329J3L plates with $\bar{\lambda}_p = 0.9$ and 1.1 , $\alpha = 4.0$, and $\sigma_{rt} = 0.9\sigma_{0.2}$ and $1.0\sigma_{0.2}$ are shown in Fig. 8 (b).

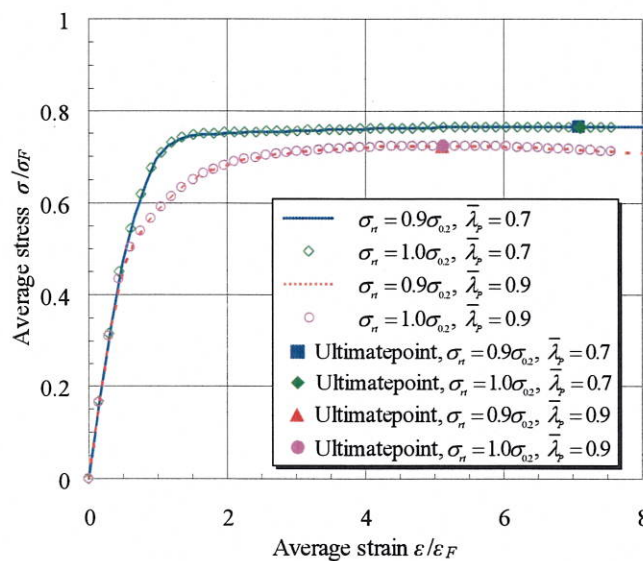
This figure shows that the non-dimensional average stress-strain curves of plates with $\sigma_{rt} = 0.9\sigma_{0.2}$ correspond to those with $\sigma_{rt} = 1.0\sigma_{0.2}$. Moreover, it is confirmed that the difference in residual stress scarcely affects the compressive behaviour of any plates except those that also have values of $\bar{\lambda}_p = 0.9$ and 1.1 and $\alpha = 4.0$ as well as simply supported plates. Thus, in the discussion, the value of $\sigma_{rt} = 0.9\sigma_{0.2}$ has been adopted for outstanding SUS329J3L plates.

4.2 Comparison of compressive behaviour

The compressive behaviour of plates made from SUS329J3L and SM570 is discussed here, focusing on the



(a) Simply supported plate ($\alpha = 1.0$)

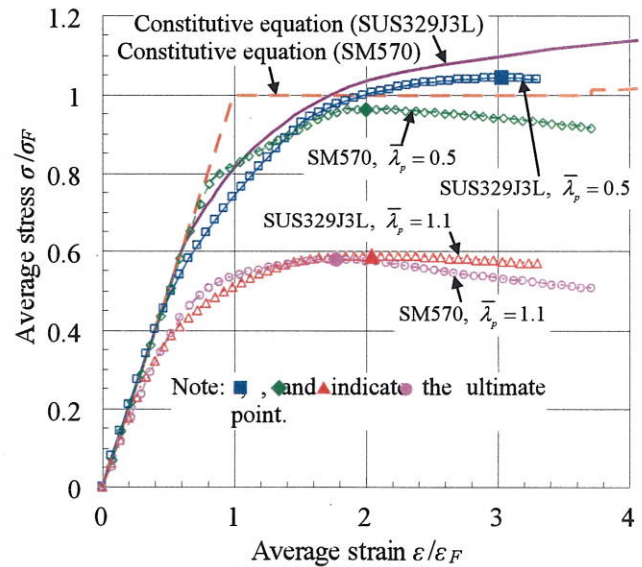


(b) Outstanding plate ($\alpha = 4.0$)

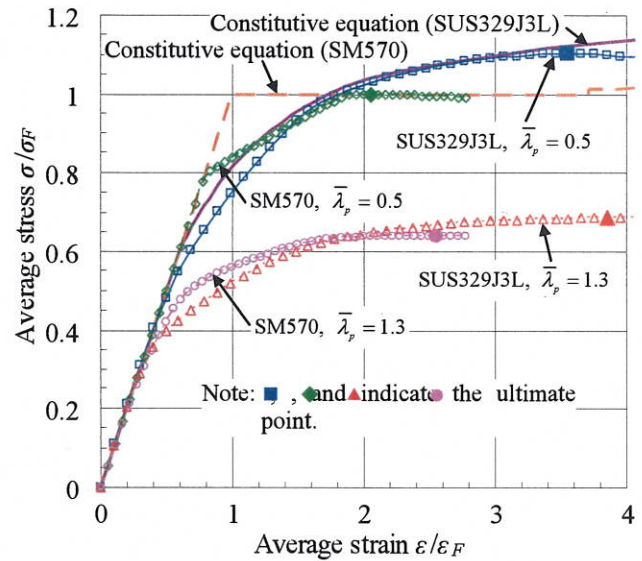
Fig. 8. Effect of residual stress of SUS329J3L plates on compressive behaviour

average stress-strain relationship and the average tangent modulus. The relationships between the non-dimensional average stress and strain of simply supported plates with values of $\alpha = 1.0$ and $\bar{\lambda}_p = 0.5$ and 1.1 , and outstanding plates with values of $\alpha = 4.0$ and $\bar{\lambda}_p = 0.5$ and 1.3 are shown in Figs. 9 (a) and (b) respectively. Non-dimensional constitutive equations for SUS329J3L and SM570 are also given in Fig. 9. This figure shows that the ultimate compressive strength of SUS329J3L plates is higher than that of SM570. Moreover, it was found that due to the effect of compressive residual stress, the non-linear behaviour of SUS329J3L and SM570 plates with $\bar{\lambda}_p = 0.5$ initiates at $\sigma/\sigma_F = 0.5$ and 0.8 respectively, and the tangential stiffness of SUS329J3L plates reduces gradually compared with SM570 plates.

Figs. 10 (a) and (b) show the relationships between the non-dimensional tangent modulus E_T/E and the non-dimensional average strain $\varepsilon/\varepsilon_F$ of simply supported and outstanding plates respectively, where the tangent modulus E_T is defined as the tangent of the average stress-strain relation



(a) Simply supported plate ($\alpha = 1.0$)



(b) Outstanding plate ($\alpha = 4.0$)

Fig. 9. Comparison of the compressive behaviour of SUS329J3L with that of SM570

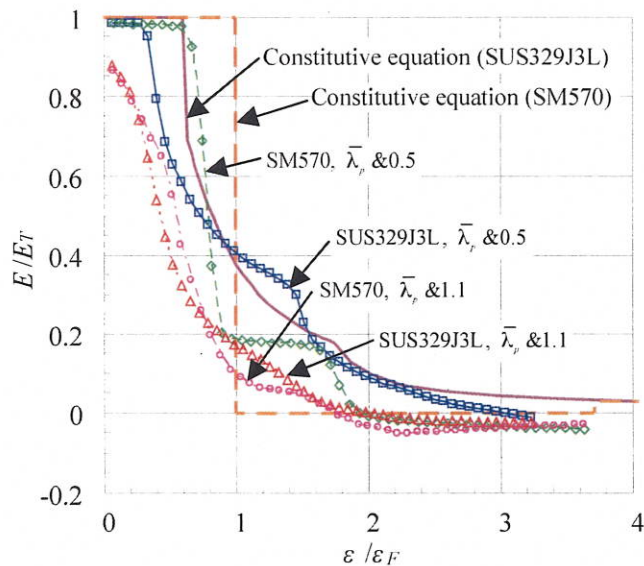
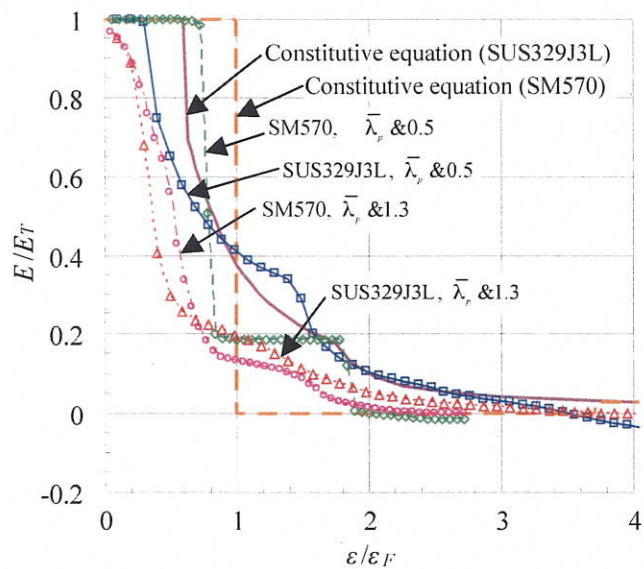
(a) Simply supported plate ($\alpha = 1.0$)(b) Outstanding plate ($\alpha = 4.0$)

Fig. 10. Relationships between non-dimensional tangent modulus and average strain

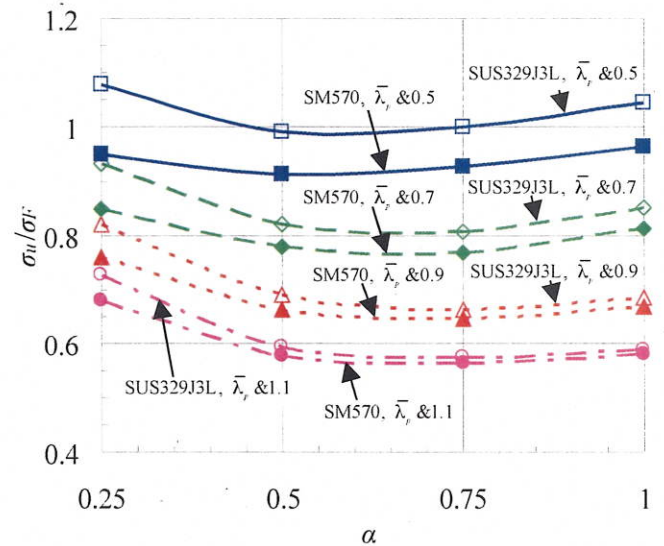
in each incremental step. In Fig. 10 it can be seen that the gradual reduction of the tangent stiffness of SUS329J3L plates is brought about by the nature of the roundhouse-shaped stress-strain curve, whereas the reduction for SM570 plates is drastic due to the yield plateau. As a result, it can be concluded that the ultimate compressive strength of SUS329J3L plates is higher than that of SM570 plates.

4.3 Effect of aspect ratio

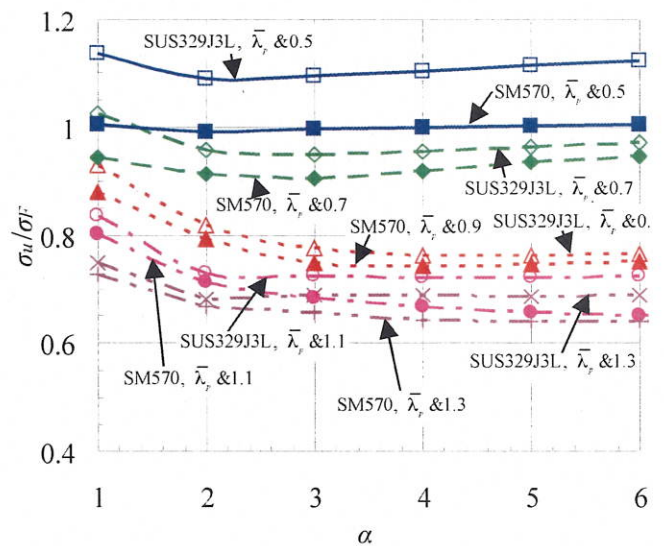
Here, the effect of aspect ratio on the ultimate compressive strength of simply supported and outstanding plates made from SUS329J3L is discussed in comparison with that of SM570.

4.3.1 Simply supported plates

Fig. 11 (a) shows the relationship between the non-dimensional ultimate compressive strength σ_u/σ_F and the aspect



(a) Simply supported plate



(b) Outstanding plate

Fig. 11. Relationships between non-dimensional ultimate strength and aspect ratio

ratio α for simply supported plates. In this figure the ultimate compressive strength of SUS329J3L plates with $\bar{\lambda}_p = 0.5$ reaches a minimum at $\alpha = 0.5$, and the ultimate compressive strength of SUS329J3L plates with $\bar{\lambda}_p = 0.7, 0.9$ and 1.1 reaches a minimum at $\alpha = 0.75$. This tendency of SUS329J3L plates is also seen in SM570 plates. Thus, the effect of aspect ratio on the ultimate compressive strength of SUS329J3L plates is similar to that of SM570.

4.3.2 Outstanding plates

Fig. 11 (b) shows the relationship between the non-dimensional ultimate compressive strength σ_u/σ_F and the aspect ratio α for outstanding plates. In this figure, except for SM570 plates with values of $\bar{\lambda}_p = 1.1$ and 1.3 , the ultimate compressive strength reaches a minimum at $\alpha = 2.0, 3.0$ and 4.0 for SUS329J3L and SM570 plates with values of $\bar{\lambda}_p = 0.5, 0.7$ and 0.9 respectively. Accordingly, the effect of aspect ratio on the ultimate compressive strength of

SUS329J3L plates with values of $\bar{\lambda}_p = 0.5, 0.7$ and 0.9 is similar to that of SM570 plates. The ultimate compressive strength of SUS329J3L plates with values of $\bar{\lambda}_p = 1.1$ and 1.3 reaches a minimum at $\alpha = 4.0$ and 5.0 respectively. On the other hand, for SM570 plates with values of $\bar{\lambda}_p = 1.1$ and 1.3 , the minimum value of the ultimate compressive strength is not clear from $\alpha = 1.0$ to 6.0 , but converges to an almost constant value at $\alpha = 6.0$. Verification of analytical results through testing will be required in future work because the reason for this was not clear in the present study.

4.4 Ultimate compressive strength and ductility

In this study the average strain at the ultimate point ϵ_u was defined as the index of ductility, and the ultimate compressive strength and ductility of SUS329J3L and SM570 plates were compared in relative terms.

Here, $(\sigma_u/\sigma_F)_{SUS}$ and $(\sigma_u/\sigma_F)_{SM}$ denote the non-dimensional ultimate compressive strength of SUS329J3L

and SM570 plates respectively. Moreover, $(\epsilon_u/\epsilon_F)_{SUS}$ and $(\epsilon_u/\epsilon_F)_{SM}$ express the ductility of each type of plate respectively. Thus, $(\sigma_u/\sigma_F)_{SUS}/(\sigma_u/\sigma_F)_{SM}$ indicates the ratio of the ultimate compressive strength of SUS329J3L plates to that of SM570 plates, and $(\epsilon_u/\epsilon_F)_{SUS}/(\epsilon_u/\epsilon_F)_{SM}$ indicates the ratio of the ductility of SUS329J3L plates to that of SM570 plates. Figs. 12 (a) and (b) show the relationships between the parameters $(\sigma_u/\sigma_F)_{SUS}/(\sigma_u/\sigma_F)_{SM}$ and $(\epsilon_u/\epsilon_F)_{SUS}/(\epsilon_u/\epsilon_F)_{SM}$ with regard to simply supported and outstanding plates respectively. Moreover, the diagonal lines plotted in Figs. 12 (a) and (b) indicate that the ultimate compressive strength and ductility of SUS329J3L and SM570 plates are equivalent, and the symbols in Fig. 12 are based on all analytical results in this study.

In Fig. 12 it can be seen that the ultimate compressive strength of all SUS329J3L plates is higher than that of all SM570 plates, and that the ductility of SUS329J3L plates is greater than that of SM570 plates. In particular, the ductility of SUS329J3L plates tends to increase as the slenderness parameter decreases. This is thought to be because SUS329J3L plates undergo significant deformation due to the nature of the roundhouse-shaped stress-strain relationship until the ultimate state is reached, whereas many SM570 plates fail without work-hardening. For outstanding plates with values of $\bar{\lambda}_p = 0.9$ and 1.1 in particular, the ductility of SUS329J3L plates is between 3.0 and 12.5 times that of SM570. Thus, SUS329J3L plates exhibit excellent ductility in comparison with that of SM570 plates, but it seems that detailed consideration is required when using SUS329J3L plates for members with limited deformation.

5 Comparison of ultimate strength curves

The ultimate compressive strength obtained from the numerical analysis was compared with the ultimate strength curves indicated by several design specifications.

5.1 Simply supported plates

The minimum ultimate compressive strength values of plates with $\bar{\lambda}_p = 0.5$ to 1.1 are plotted in Fig. 13 (a). Also shown in Fig. 13 (a) are the ultimate strength curves for the plate made from mild carbon steel proposed by Nara et al. [20], and the ultimate strength curve of the plate specified by the European design standard for stainless steel structures (EN 1993-1-4) [21].

From this figure, in line with the analytical results, it can be seen that the difference in the ultimate compressive strength between SUS329J3L and SM570 plates increases as the slenderness parameter decreases. Moreover, the curve proposed by Nara et al. [20] estimates the ultimate compressive strength for SUS329J3L plates conservatively, assuming values of $\bar{\lambda}_p = 0.5$ and 0.7 , even though this is a curve for carbon steel plates. On the other hand, the curve for stainless steel plates specified by EN 1993-1-4 [21] overestimates the ultimate compressive strength of all SUS329J3L plates.

5.2 Outstanding plates

The minimum ultimate compressive strengths of outstanding plates with $\bar{\lambda}_p = 0.5$ to 1.3 are plotted in Fig. 13 (b). Also

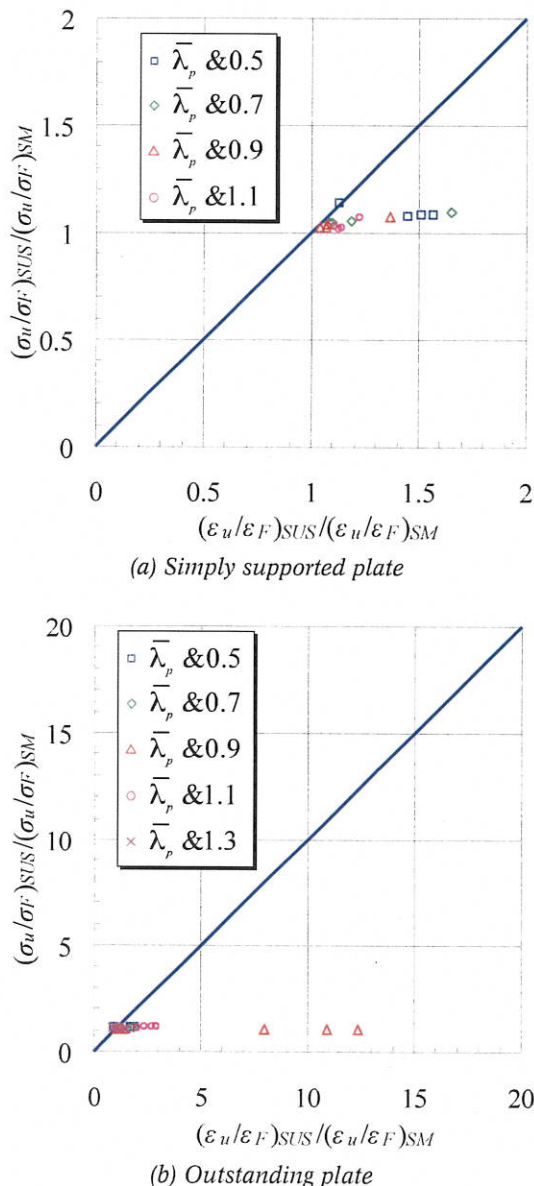


Fig. 12. Relationships between ultimate strength ratio and ultimate strain ratio

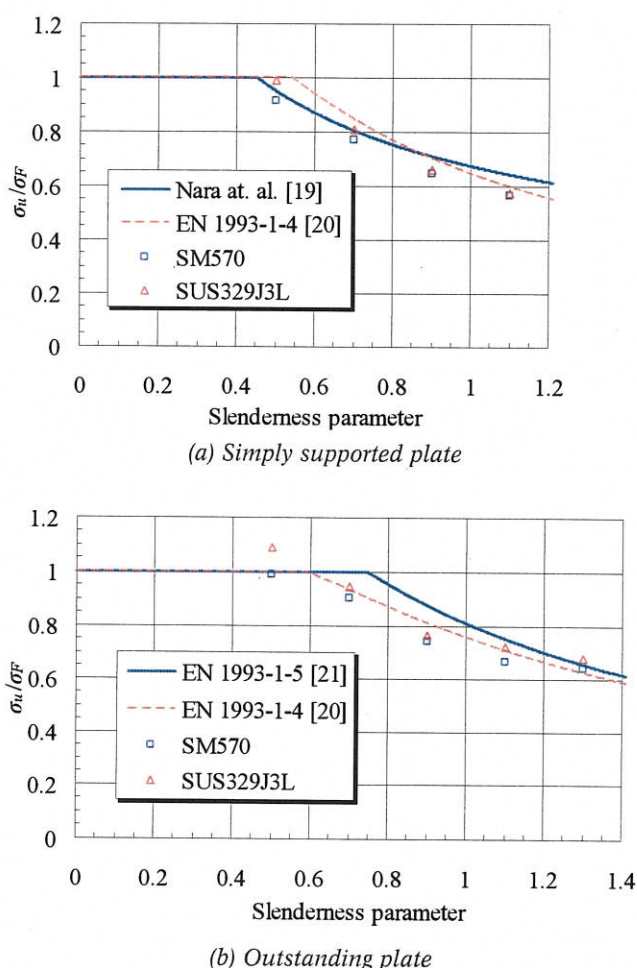


Fig. 13. Comparing the ultimate compressive strength with the curves

shown in Fig. 13 (b) are the ultimate strength curves for outstanding plates specified by the European design standard for carbon steel structures (EN 1993-1-5) [22] and stainless steel structures (EN 1993-1-4) [21].

This figure shows that the difference in the ultimate compressive strength between SUS329J3L and SM570 plates reaches a minimum at $\lambda_p = 0.9$ according to the analytical results. Moreover, the curve for EN 1993-1-4 estimates the ultimate compressive strength of the plate with values of $\lambda_p = 0.5, 0.7, 1.1$ and 1.3 . On the other hand, because of the ultimate strength curve for carbon steel plates, the curve of EN 1993-1-5 overestimates the ultimate compressive strength of SUS329J3L plates with values of $\lambda_p = 0.7, 0.9$ and 1.1 .

In future work, the compatibility of ultimate strength curves needs to be discussed using statistical data based on measured results of initial imperfections because in this study it is discussed using analytical data only.

6 Conclusions

Based on coupon test results, this study confirms the applicability of the existing constitutive equation for SUS329J3L duplex stainless steel. In order to ascertain the compressive behaviour of simply supported and outstanding plates made from SUS329J3L and SM570, a numerical

analysis was also conducted. The results can be summarized as follows:

- (1) The difference in residual stress assumed in this study scarcely affects the ultimate compressive strength of SUS329J3L plates.
- (2) The compressive behaviour of SUS329J3L plates heavily depends on the stress-strain curve.
- (3) The minimum ultimate compressive strength of simply supported SUS329J3L plates with a slenderness parameter of 0.5 appears at 0.5 in aspect ratio.
- (4) The minimum ultimate compressive strength of simply supported SUS329J3L plates with slenderness parameters of 0.7, 0.9, and 1.1 appears at 0.75 in aspect ratio.
- (5) The minimum ultimate compressive strength of outstanding SUS329J3L plates with slenderness parameters of 0.5, 0.7, 0.9, 1.1 and 1.3 appears at 2.0, 3.0, 4.0, 5.0 and 5.0 in aspect ratio respectively.
- (6) The ultimate compressive strength and ductility of SUS329J3L plates are greater than those of SM570.
- (7) The ultimate strength curve for simply supported stainless steel plates specified by EN 1993-1-4 overestimates the ultimate compressive strength of all SUS329J3L plates in this study.
- (8) The ultimate strength curve for outstanding stainless steel plates specified by EN 1993-1-4 evaluates the ultimate compressive strength of all SUS329J3L plates conservatively, except for the plate with a slenderness parameter of 0.9.

References

- [1] Stainless Steel Building Association of Japan: Concept of the LCC and introduction of an application case of stainless steel (LCC series, No. 3), *Stainless Steel Structure*, pp. 17–20, December 1998. (in Japanese).
- [2] Sobrino, J. A.: Stainless steel road bridge in Menorca, Spain. *Structural Engineering International*, pp. 96–100, February 2006.
- [3] Stainless Steel Building Association of Japan: Design and construction standards for stainless steel buildings, SSBA, Tokyo, Japan, 1995. (in Japanese).
- [4] Matsushita, H., Iwata, S., Arizumi, S., Yabuki, T.: A study on the ultimate compressive strength of stainless steel plates stiffened with mild carbon steel ribs. *Journal of Structural Engineering, JSCE*, vol. 49 A, pp. 833–844, 2003. (in Japanese).
- [5] Matsushita, H., Yabuki, T., Arizumi, Y., Iwata, S.: An experimental study on the shear buckling strength of stainless steel web plates in I-girders. *Journal of Structural Engineering, JSCE*, vol. 50 A, pp. 799–808, 2004 (in Japanese).
- [6] Matsushita, H., Yabuki, T., Arizumi, Y., Iwata, S.: Ultimate strength of stainless steel plates under shear. *Journal of Structural Engineering, JSCE*, vol. 52 A, pp. 865–874, 2006 (in Japanese).
- [7] Kuwamura, H., Kato, T.: Local buckling of chromium stainless steel compressive members – Study on lightweight stainless steel structures Part 5. *Journal of Structural and Construction Engineering, Transactions of AIJ*, No. 582, pp. 163–170, 2004 (in Japanese).
- [8] Euro Inox and The Steel Construction Institute: Design Manual for Structural Stainless Steel (2nd ed.), 2002.
- [9] Burgan, B. A., Baddoo, N. R., Gilsenan, K. A.: Structural design of stainless steel members – comparison between Eurocode 3 Part 1.4 and test results. *Journal of Constructional Steel Research, Science Direct*, vol. 54, pp. 51–73, 2000.
- [10] Miyazaki, Y., Miyoshi, T., Ochi, N., Mori, S., Nara, S.: Ultimate Compressive Strength and Ductility of Austenitic Stain-

- less Steel Plate. 7th German-Japanese Bridge Symposium (CD-ROM), Osaka, Japan, 2007.
- [11] Miyoshi, T., Miyazaki, Y., Nara, S.: Ultimate compressive behaviour of simply supported SUS329J3L stainless steel plates. *Journal of Construction Steel*, vol. 16, pp. 47–52, 2008 (in Japanese).
- [12] Miyoshi, T., Miyazaki, Y., Nara, S.: A Constitutive Equation for Ferritic Stainless Steel and Ultimate Strength of Compressive Plates of SUS410 L. 7th German-Japanese Bridge Symposium (CD-ROM), Osaka, Japan, 2007.
- [13] Crisfield, M. A.: Non-linear finite element analysis of solids and structures vol. 1: Essentials. John Wiley & Sons, 1991.
- [14] Nara, S.: Steel properties for improvement in ultimate strength and ductility of longitudinally stiffened plates under uniaxial compression. *Proc. of Annual Technical Session, SSRC*, pp. 219–224, 1994.
- [15] Komatsu, S., Nara, S.: Statistical study on steel plate members. *Journal of Struct. Engng. Proc. of ASCE*, vol. 109, No. 4, pp. 977–992, Apr., 1983.
- [16] Japan Road Association, Specifications and Commentary for Highway Bridges Part I, Tokyo, Japan, 2002 (in Japanese).
- [17] Komatsu, S., Kitada, T.: Ultimate strength characteristics of outstanding steel plates with initial imperfections under compression. *Proc. of JSCE*, No. 314, pp. 15–26, 1981 (in Japanese).
- [18] Nakatani, M., Matsushita, H., Yabuki, T., Arizumi, Y.: Estimation of the welding residual stress of stainless steel outstanding plates. *Proc. of Annual Technical Session 1, JSCE*, pp. 913–914, 2005 (in Japanese).
- [19] Komatsu, S., Ushio, M., Kitada, T.: An experimental study on the residual stress and initial deformations of stiffened plates. *Proc. of JSCE*, No. 265, pp. 25–35, 1977 (in Japanese).
- [20] Nara, S., Fukumoto, Y.: Étude statistique de la résistance ultime des plaques en acier sollicitées dans leur plan. *Construction Métallique*, No. 3, pp. 15–24, 1991.
- [21] European Committee for Standardization, CEN. Eurocode 3: Design of steel structures – Part 1–4: General rules – Supplementary rules for stainless steels, CEN, European Standard, EN 1993-1-4, 2006.
- [22] European Committee for Standardization, CEN. Eurocode 3: Design of steel structures – Part 1–5: Plated structural elements, CEN, European Standard, EN 1993-1-5, 2006.
- Keywords:** SUS329J3L duplex stainless steel; ultimate strength of compressive plates; ductility; elasto-plastic finite displacement analysis; compound *Ramberg-Osgood* curve; tangent modulus
- Authors:**
Research Associate Takao Miyoshi, Researcher Yasuhiro Miyazaki, and Professor Satoshi Nara, Osaka University, Osaka, Japan